***JKPK (JURNAL KIMIA DAN PENDIDIKAN KIMIA)**, Vol. 11, No. 1, 2026* *pp. 60-75*
*Chemistry Education Study Program, Universitas Sebelas Maret* *ISSN 2503-4146*
*https://jurnal.uns.ac.id/jkpk* *ISSN 2503-4154 (online)*

# Isolation and Characterization of Cellulose from Golden Melon (*Cucumis melo L.*) Fruit Peel Using Microwave-Assisted Extraction

**Nurul Fadilah[1], Henny Purwaningsih[1,2*], Tetty Kemala[1]**

*[1]Department of Chemistry, Faculty of Mathematics and Natural Sciences, IPB University, Bogor, Indonesia*
*[2]Integrated Laboratory, IPB University, Bogor, Indonesia*

**ABSTRACT**

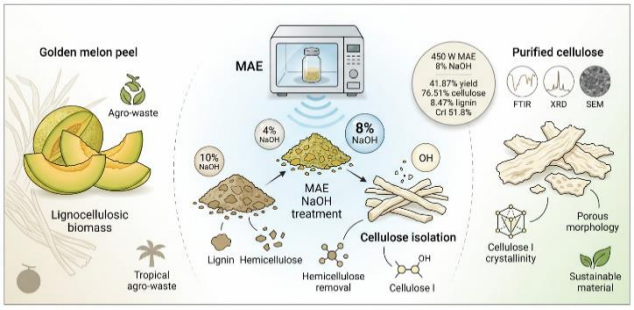


Golden melon (Cucumis melo L.) peel represents a promising source of cellulose derived from agricultural by-products. This study aimed to identify a favorable NaOH concentration for cellulose isolation using microwave-assisted extraction (MAE), as well as to evaluate the resulting cellulose in terms of yield, composition, and crystallinity. The extraction was conducted at 450 W using NaOH concentrations of 4%, 8%, and 10%. A relatively high cellulose yield (41.87 ± 0.16%) was obtained with 8% NaOH, accompanied by improved purity, as indicated by the relatively high cellulose content (76.51%) and low lignin content (8.47%). Fourier Transform Infrared (FTIR) analysis confirmed the presence of characteristic cellulose functional groups along with a reduction in lignin-related peaks. X-ray diffraction (XRD) analysis indicated increased crystallinity after treatment, with crystallinity indices of 52.5%, 51.8%, and 40.3% for 4%, 8%, and 10% NaOH, respectively. SEM analysis of the 8% NaOH sample showed a rough and porous morphology, likely associated with the removal of non-cellulosic components. These findings suggest that MAE is a potentially effective approach for cellulose isolation from golden melon peel, with 8% NaOH representing a favorable condition within the studied parameters based on a balance of yield, purity, and crystallinity.

**Keywords:** *Cellulose; Cucumis melo L.; Delignification; Microwave-assisted Extraction; XRD*

**Corresponding Author:* *hennypu@apps.ipb.ac.id*

**How to cite:** N. Fadilah, H. Purwaningsih, and T. Kemala, "Isolation and characterization of cellulose from golden melon (*Cucumis melo* L.) fruit peel using microwave-assisted extraction," *Jurnal Kimia dan Pendidikan Kimia (JKPK)*, vol. 11, no. 1, pp. 60-75, 2026. [Online]. Available: https://doi.org/10.20961/jkpk.v11i1.106706
*Received: 2025-08-11* *Accepted: 2026-04-23* *Published: 2026-04-30*

## INTRODUCTION

Cellulose $(C_6H_{10}O_5)_n$ is one of the most abundant natural polymers and a primary structural component of plant cell walls. It is a linear polysaccharide composed of D-glucose units linked by β-(1→4)-glycosidic bonds, forming a highly ordered structure that contributes to its mechanical strength and chemical stability. Due to its biocompatibility, biodegradability, and non-toxic nature, cellulose has been widely utilized in various industries, including biomedicine, pharmaceuticals, cosmetics, energy, paper, textiles, and food sectors [1][2]. Its abundance, renewability, and versatility make it a promising raw material for the development of sustainable and environmentally friendly materials. Cellulose can be derived from various sources, including wood, herbaceous plants, cotton, agricultural

residues, algae, bacteria, and recycled paper [3].

Agricultural by-products such as melon peels represent a promising alternative source of cellulose. Melons (*Cucumis melo* L.) are widely consumed in tropical countries, including Indonesia, with production reaching approximately 118,696 tons in 2022 [4], generating substantial quantities of peel waste. Dried melon peel is an abundant agro-industrial residue rich in carbohydrates, where cellulose constitutes a major structural component within a lignin–hemicellulose matrix [5][6]. Melon peel has been reported to contain approximately 24–28% cellulose in its raw form, which can increase to around 40–59% after pectin removal, along with substantial amounts of hemicellulose and lignin [5][7]. Such cellulose levels highlight the potential of golden melon peel as a cellulose-rich feedstock for isolation and conversion into value-added products. Nevertheless, despite this promising profile, targeted studies on cellulose extraction and characterization specifically from golden melon peel remain limited.

Adewuyi and Pereira [8] reported the only available study on cellulose isolation from golden melon skin. Their work employed a conventional alkali-based method involving prolonged heating at 80 °C for 5 hours followed by bleaching, resulting in approximately 23% cellulose yield. Although effective, this method requires extended processing time and continuous heating, and it does not systematically examine the relationship between processing conditions and cellulose quality. Microwave-assisted extraction (MAE) offers a potential alternative because it provides rapid and volumetric heating, allowing delignification and bleaching processes to be completed within minutes per stage [9]. The use of MAE for golden melon peel remains insufficiently explored, particularly regarding the effect of NaOH concentration under microwave conditions and the balance between compositional purity, lignin removal, and crystallinity of the resulting cellulose. This issue represents an important research gap compared with previous conventional treatments.

Cellulose isolation typically involves the removal of lignin and hemicellulose through delignification and bleaching processes. Among various methods, alkaline treatment plays an important role by disrupting lignin structures and solubilizing hemicellulose, thereby contributing to cellulose enrichment [9]. Under microwave irradiation, these reactions may be further enhanced due to improved heat transfer and reaction kinetics [10]. However, the effectiveness of alkali treatment strongly depends on NaOH concentration, which can influence not only lignin removal but also cellulose degradation and structural ordering [10]-[12].

Microwave-assisted heating has been applied in the isolation of cellulose from vegetable wastes [13], lignin from cocoa shells [14], and pectin from onion and garlic waste [15]. This technique transfers energy directly into the material through dipole rotation and ionic conduction, thereby enhancing reaction rates and heat distribution. As a result, microwave heating can reduce processing time, although the

extent of lignin and hemicellulose removal still depends on the intrinsic composition and structure of each biomass [10][16].

Recent studies have reported the effectiveness of MAE for cellulose isolation from various lignocellulosic biomasses. MAE applied to corn husk produced cellulose with a yield of 75.23% within 14 minutes likely due to rapid volumetric heating [9]. Similarly, alkali treatment under MAE applied to lemongrass straw was reported to yield of 37.46% with a high crystallinity index (~70%) [11]. In addition, MAE has been used to produce cellulose nanocrystals from almond shells with a crystallinity of ~56% using fewer processing steps than conventional methods [12]. These biomasses differ in initial lignin and hemicellulose contents and cell wall architecture, which may influence delignification efficiency, cellulose retention, and final crystallinity [9][10]. Therefore, these studies provide useful context for understanding how the distinct composition of golden melon peel may affect cellulose yield, lignin removal, and crystallinity when subjected to MAE.

This study aims to examine the effect of NaOH concentration under MAE on cellulose isolation from golden melon peel. Under microwave irradiation, higher NaOH concentrations may enhance lignin and hemicellulose solubilization and fiber swelling, thereby potentially increasing cellulose purity and crystallinity. However, excessive alkalinity may also promote cellulose peeling or degradation, reducing overall yield and altering the crystalline structure. Therefore, a favorable NaOH concentration was identified by evaluating the balance between cellulose yield and purity, while also examining its impact on crystallinity, along with morphological characteristics of the selected sample.

## METHODS

The research methodology comprised three main stages: preparation of golden melon peel through drying and pulverizing, cellulose isolation using microwave-assisted alkali treatment at varying NaOH concentrations, and characterization of the isolated cellulose using FTIR spectroscopy and XRD. SEM analysis was performed on the selected sample (8% NaOH). Cellulose and lignin contents were also determined.

### 1. Materials and Tools

The materials used in this study included golden melon peel, NaOH (Sigma-Aldrich), methanol (Sigma-Aldrich, 99.8%), $H_2SO_4$ (Merck, 95–97%), $H_2O_2$ (Sigma-Aldrich, 30%), glycerol, and distilled water. The equipment used comprised Pyrex glassware (beakers, measuring cylinders, stirring rods, volumetric flasks, and porcelain crucibles), microwave (Sharp R-220MA-WH Solo, 20 l, 450 W), oven, FTIR spectrometer (Bruker Alpha II), X-ray diffraction (X'Pert Malvern PANalytical), and scanning electron microscope (COXEM EM-40).

### 2. Isolation of Cellulose from Golden Melon Peel

The isolation procedure was adapted from Yupa *et al*. [9]. Golden melon peels were washed and dried in an oven at 40 °C. The dried peels were pulverized and sieved to obtain a fine powder. A total of 15 g of powder was mixed with 150 ml of a glycerol–

methanol solution (2:1, v/v) and 35 ml of 1.75% $H_2SO_4$. The mixture was stirred manually, followed by MAE at a constant power of 450 W for 3 minutes. This process was conducted in an open vessel. After irradiation, the mixture was directly filtered without any intentional cooling interval, and the residue was dried in an oven at 105 °C.

The dried residue was then treated with NaOH solutions at concentrations of 4%, 8%, and 10%, followed by MAE at 450 W for 3 minutes under the same conditions (pre-stirring, open vessel, and immediate filtration after irradiation). The mixture was filtered and washed with distilled water until neutral pH was achieved. Subsequently, the residue was bleached using 10% $H_2O_2$ and subjected to MAE at 450 W for 4 minutes per cycle under the same conditions. The bleaching process was repeated twice sequentially. After completing all bleaching cycles, the residue was washed with distilled water until neutral pH was achieved. The final product was dried in an oven at 60 °C until a constant weight was obtained. The resulting cellulose was then used for further characterization.

### 3. Determination of Cellulose and Lignin Content

Cellulose content was determined based on ASTM D1103-60 [17] and lignin content was determined using the Klason method according to SNI 8429:2017 [18]. Both analyses were carried out once (without analytical replicates) by an accredited external laboratory following the respective standard procedures. Therefore, the reported cellulose and lignin contents represent single measured values and should be interpreted as approximate indicators rather than statistically robust estimates.

### 4. Functional Groups Analysis

Functional group analysis was carried out using an FTIR spectrometer (Bruker Alpha II). The samples were ground, mixed with KBr, and pressed into pellets under high pressure. The spectra were recorded in the wavenumber range of 4000–600 $cm^{-1}$ with a spectral resolution of 8 $cm^{-1}$ and 24 scans.

### 5. Crystallinity Analysis

The crystalline structure of the isolated cellulose was analyzed using an XRD (X'Pert Malvern PANalytical) with Cu Kα radiation (λ = 1.5406 Å) operated at 40 kV and 15 mA. The diffraction patterns were recorded over a 2θ range of 10–50°.

The crystallinity index (CrI) was calculated using the Segal method as shown in Equation (1),

$$CrI = (I_{002} - I_{am}) / I_{002} \times 100\% \quad (1)$$

where $I_{002}$ is the maximum intensity of (002) crystalline plane at 2θ ≈ 22° and $I_{am}$ is the intensity of amorphous region at 2θ ≈ 18°.

### 6. Morphology Analysis

The morphology of the selected sample was examined using a scanning electron microscope (COXEM EM-40). The sample was mounted on aluminum stubs using double-sided carbon tape and observed under an accelerating voltage of 12 kV, a working distance of 32.5 mm, and a spot size of 6. Observations were conducted at a magnification of 100× to provide a general overview of surface morphology and to visualize larger-scale surface features in

the treated cellulose. Only the sample treated with 8% NaOH was selected for SEM observation, as this condition was considered a favorable based on an integrative assessment of cellulose yield, compositional indicators (cellulose and lignin content), and crystallinity. Due to the limited magnification, the results are interpreted as qualitative observations of macro-scale surface features and do not represent detailed microstructural characterization or all treatment conditions.

### 7. Data Analysis

Cellulose yield experiments were conducted in triplicate and the results are presented as mean ± standard deviation. Statistical analysis was performed using the Kruskal-Wallis test, followed by Dunn's post hoc test to evaluate differences among NaOH concentrations. Cellulose and lignin contents were determined using standardized methods by an external laboratory and are reported as single measured values, without replication. These single-value compositional data were therefore used descriptively and not subjected to statistical testing. FTIR, XRD, and SEM analyses were used to characterize the isolated cellulose. FTIR and SEM results were interpreted qualitatively, whereas XRD data were used to estimate the crystallinity index, without statistical analysis.

A favorable NaOH concentration was selected based on an integrative assessment using the following criteria: among conditions with no statistically lower cellulose yield, the one exhibiting higher cellulose content and lower lignin content (based on single measurements) was considered the most favorable. Crystallinity index values were used as a complementary, semi-quantitative indicator of structural order.

## RESULTS AND DISCUSSION

### 1. Cellulose of Golden Melon Peel

The isolation of cellulose from golden melon peel using MAE was completed within 14 minutes through three sequential steps: liquefaction, delignification, and bleaching. This duration is markedly shorter than that reported for conventional methods used by Adewuyi and Pereira, which typically require over 5 hours for delignification and an additional 10 hours for bleaching, totaling approximately 15 hours [8]. This reduction in processing time may be attributed to the rapid and uniform thermal energy distribution generated by microwave heating, which can enhance reaction kinetics and mass transfer efficiency [10][19]. These findings indicate that MAE can reduce the processing time for cellulose isolation from golden melon peel. However, the overall advantages of this process cannot yet be conclusively established, as its energy efficiency and scalability have not been directly measured and require further evaluation.

The isolation process began with a liquefaction step, which was performed for 3 minutes using a mixture of glycerol and methanol as organic solvents, with sulfuric acid as the catalyst. This combination may provide a synergistic effect, where glycerol acts as a plasticizing and swelling agent that penetrates the cellulose matrix, while methanol enhances the solubilization of extractives and non-cellulosic components such as waxes, pigments, lipids, and tannins [9]. The presence of sulfuric acid facilitates

the cleavage of β-(1→4)-glycosidic bonds in carbohydrate components, leading primarily to the depolymerization of hemicellulose in amorphous regions [20].

The brown coloration of the liquefied product (Figure 1b) suggests the dissolution of these impurities and the formation of degradation products such as furfural and hydroxymethylfurfural (HMF), which are commonly associated with carbohydrate hydrolysis [21]. This process may increase the accessibility of cellulose for subsequent delignification and bleaching. Furthermore, the removal of amorphous components may contribute to an increase in relative crystallinity, although this effect depends on the extent of their removal [22][23].


**Figure 1.** The physical appearance of (a) raw material, (b) liquefaction result, (c) delignification result, and (d) bleaching result.

The process was followed by a delignification stage aimed at removing lignin as well as residual pectin and hemicellulose, thereby improving the accessibility of cellulose within the biomass matrix [9]. Sodium hydroxide (NaOH) was used as the delignification agent at concentrations of 4%, 8%, and 10%, and the treatment was carried out for 3 minutes under microwave irradiation.

Lignin removal is generally attributed to the nucleophilic attack of hydroxide ions ($OH^-$) on ester and ether linkages, particularly the β-O-4 aryl ether bonds, which are the predominant linkages in lignin [24]. The cleavage of these bonds may lead to lignin depolymerization into smaller phenolic fragments, which can subsequently form water-soluble sodium phenolate salts, allowing their separation from the cellulose fraction (Figure 2) [16][25].

The resulting material exhibited a light brown color (Figure 1c), suggesting that lignin removal was substantial but not complete, as residual chromophoric compounds remained in the fiber matrix [16]. Therefore, a bleaching step was required to further remove these components and improve cellulose quality.

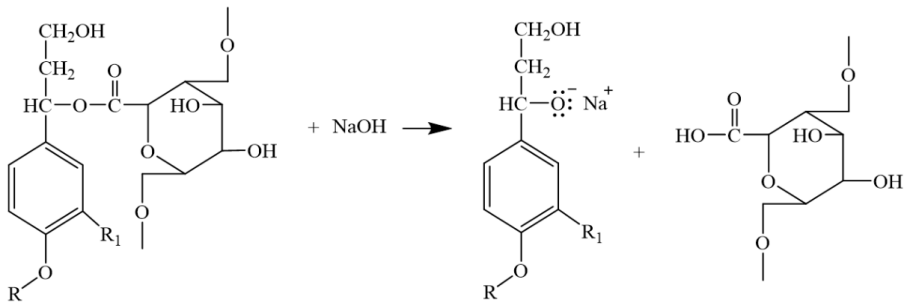


**Figure 2.** Lignin removal reaction using NaOH.

The color change after bleaching (Figure 1d) indicates the removal of residual pigments and non-cellulosic impurities. Hydrogen peroxide, an eco-friendly and

effective oxidizing agent [26], was used in this stage. Under alkaline conditions, hydrogen peroxide generates reactive perhydroxyl anions ($HOO^-$), which are known to be responsible for the oxidation of lignin chromophores (Equation 2) [9]. These species disrupt conjugated structures that are responsible for the residual color of the sample.

$$H_2O_2 + OH^- \rightarrow HOO^- + H_2O \quad (2)$$

The effect of NaOH concentration on cellulose yield is shown in Table 1. The yield increased from 32.56 ± 0.24% at 4% NaOH to 41.87 ± 0.16% at 8%, followed by a slight decrease at 10% (41.52 ± 0.24%), although the difference between 8% and 10% was not statistically significant. This trend indicates a favorable alkaline range for cellulose recovery, under the applied conditions, rather than a sharply defined optimum based on yield alone.

**Table 1.** Cellulose yield obtained from golden melon peel at different NaOH concentrations (4%, 8%, and 10%) using MAE.

| [NaOH] | Cellulose yield (%) |
|---|---|
| 4% | 32.56 ± 0.24$^{b}$ |
| 8% | 41.87 ± 0.16$^{a}$ |
| 10% | 41.52 ± 0.24$^{ab}$ |

Notes: Data with different letters in the column indicate significant differences ($p$ <0.05).

The cellulose yield obtained under the selected MAE condition reached 41.87 ± 0.16%, which is approximately 18.87 percentage points higher than the yield reported by Adewuyi and Pereira [8]. This result suggests that MAE may enhance cellulose recovery under the applied conditions, potentially due to rapid and uniform internal heating [16],[19].

This cellulose yield trend is consistent with alkaline pretreatment of lignocellulosic biomass reported in previous studies, where increasing alkali concentration enhances delignification by cleaving lignin–carbohydrate linkages and solubilizing non-cellulosic components [27]–[29]. For example, CaO pretreatment of corn stover at higher concentrations improves the disruption of lignin–hemicellulose–cellulose interactions, resulting in increased cellulose availability [29]. However, at higher alkaline severity, cellulose degradation may occur through peeling reactions and alkaline hydrolysis, leading to reduced yield [30][31]. A similar trend has been observed in other pretreatment systems, where extensive lignin removal is accompanied by increased biomass loss [32]. These findings suggest that 8% and 10% NaOH fall within a favorable range for cellulose recovery, as no significant difference in yield was observed. However, 8% NaOH provides a more favorable balance when compositional factors (cellulose and lignin content) are considered, as further discussed in the following section.

## 2. Impact of NaOH Concentration on Cellulose Purity

NaOH treatment under microwave-assisted conditions influenced the cellulose and lignin contents of golden melon peel. Cellulose content increased from 29.87% in the raw material to 73.88%, 76.51%, and 72.44% after treatment with 4%, 8%, and 10% NaOH, respectively. These values indicate approximately 2.4–2.6-fold

enrichment in α-cellulose compared with the raw material. Lignin content decreased from 19.14% in the raw material to 10.12%, 8.47%, and 10.76% after treatment with 4%, 8%, and 10% NaOH, respectively, corresponding to lignin removal efficiencies of 47.1%, 55.8%, and 43.8% (Figure 3).

A combination of high cellulose content and low lignin content was observed at 8% NaOH, indicating a potentially favorable alkali concentration that may effectively disrupt lignin–carbohydrate complexes without causing excessive cellulose degradation. At 10% NaOH, the slightly lower cellulose content may be attributed to partial cellulose degradation [30][31]. However, as these measurements were obtained as single values, the observed differences should be interpreted as indicative trends rather than definitive quantitative differences.

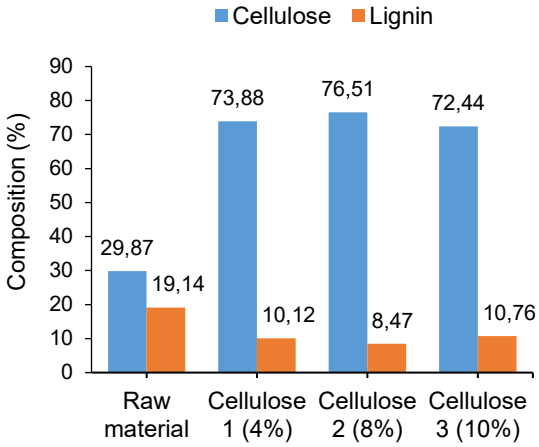


**Figure 3.** Effect of NaOH concentration on cellulose and lignin content.

The NaOH concentrations used (4%, 8%, and 10%) are consistent with previous study reporting favorable lignin solubility under similar alkaline conditions [33]. The lignin removal observed in this study (43.8–55.8%) may suggest relatively more effective delignification under microwave irradiation. In comparison, the conventional method reported in [33] showed lignin removal ranging from 5.8–10.4%. However, such comparisons should be interpreted with caution due to differences in experimental conditions.

Compared with a previous MAE study on corn husk, which reported lignin removal of up to ~90% using 10% NaOH [9], the lignin removal observed in this study was lower. Nevertheless, a higher cellulose content was obtained (up to 76.51%) compared to 72.1% reported in that study. These observations suggest that the extent of lignin removal alone may not fully determine cellulose enrichment, and that differences in biomass characteristics, such as structural composition and lignin distribution, may also play a role.

### 3. FTIR Characterization of Cellulose

The success of cellulose isolation was evaluated using FTIR spectroscopy to identify functional groups in the samples. The spectra of the raw material and cellulose isolated at different NaOH concentrations (4%, 8%, and 10%) are shown in Figure 4. In the raw material, characteristic peaks associated with lignin and hemicellulose appeared at 1240, 1512, and 1732 $cm^{-1}$, corresponding to C–O and C–O–C stretching of aryl ethers, aromatic skeletal vibrations (C=C stretching), and C=O stretching of acetyl or ester groups, respectively [34]. After alkali treatment under MAE, these peaks reduced or disappeared, indicating the removal of non-cellulosic components. Minor residual peaks were still observed at 1251 and 1731 $cm^{-1}$ in Cellulose 1 (NaOH 4%) and

at 1259 and 1731 $cm^{-1}$ in Cellulose 2 (NaOH 8%), while Cellulose 3 (NaOH 10%) showed only a weak band around 1263 $cm^{-1}$.

The absorption band at 1263–1240 $cm^{-1}$ is attributed to C–O and C–O–C vibration of aryl ether in lignin and acetyl groups in hemicellulose. The reduction in its intensity after treatment suggests partial removal of these non-cellulosic components. In addition, the peak at approximately 1512 $cm^{-1}$ was no longer observed in all cellulose samples, indicating significant lignin reduction following alkali treatment under MAE [35].

The disappearance of the approximately 1731 $cm^{-1}$ band in Cellulose 3 indicates the removal of acetyl groups in hemicellulose and the cleavage of ester bonds within lignin–carbohydrate complexes at higher NaOH concentration. This band primarily represents ester functional groups rather than the entire lignin structure. Its disappearance therefore reflects hemicellulose removal and disruption of lignin–carbohydrate linkages, rather than complete lignin elimination [36].

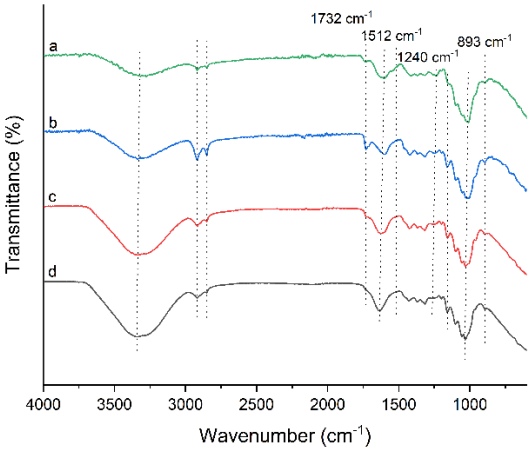


**Figure 4.** FTIR spectra of (a) raw material, (b) Cellulose 1 (NaOH 4%), (c) Cellulose 2 (NaOH 8%), and (d) Cellulose 3 (NaOH 10%).

This interpretation is supported by compositional analysis, where Cellulose 2 shows lower lignin content and higher cellulose fraction than Cellulose 3. This discrepancy suggests that the removal of specific functional groups does not necessarily correspond directly to overall lignin content. Therefore, although Cellulose 3 exhibits more extensive cleavage of ester bond, it does not represent the lowest lignin fraction. Instead, Cellulose 2 may be considered the most favorable condition under the applied criteria, given its compositional purity and relatively high cellulose yield. These findings highlight that FTIR analysis is inherently qualitative or semi-quantitative and should be integrated with quantitative compositional data to prevent overinterpretation of spectral features [37].

Regarding the characteristic cellulose peaks, all samples exhibited a strong absorption band at approximately 893–895 $cm^{-1}$, corresponding to the inter-unit C–O–C stretching vibration of anhydroglucose, which is indicative of β-(1→4)-glycosidic linkages in cellulose [38]. Similar peaks have been reported at 903 $cm^{-1}$ in cellulose from corn husks [9] and at 895 $cm^{-1}$ in cellulose derived from banana stems [16].

Other typical cellulose absorptions were also observed, including C–O stretching vibrations in range of 1030–1025 $cm^{-1}$ [9], C–O–C asymmetric stretching of the pyranose ring at around 1161 $cm^{-1}$ [35], O–H bending vibrations at 1633–1623 $cm^{-1}$, C–H stretching of alkanes at 2918–2848 $cm^{-1}$, and a broad O–H stretching band of hydrogen-bonded

hydroxyl groups at 3339–3318 $cm^{-1}$ [16]. These consistent spectral features, as summarized in Table 2, confirm that the isolated samples retain the fundamental cellulose structure while showing substantial removal of non-cellulosic components.

**E 2.** Wavenumbers of FTIR spectra of raw material and cellulose at NaOH 4%, 8%, and 10% concentration.

| Wavenumber ($cm^{-1}$) | | | | Functional group |
|---|---|---|---|---|
| Raw material | Cellulose 1 (NaOH 4%) | Cellulose 2 (NaOH 8%) | Cellulose 3 (NaOH 10%) | |
| 893 | 893 | 895 | 895 | C-O-C at β-1,4-glycosidic |
| 1011 | 1020 | 1031 | 1031 | C-O of pyranose |
| 1156 | 1158 | 1159 | 1159 | C-O-C of pyranose |
| 1240 | 1251 | 1259 | 1263 | C=O of hemicellulose and lignin, C-O-C aromatic ether of lignin |
| 1512 | - | - | - | C=C aromatic of lignin |
| 1602 | 1602 | 1631 | 1633 | O-H bending of cellulose |
| 1732 | 1731 | 1731 | - | C=O at hemicellulose and lignin |
| 2848 | 2850 | 2850 | 2850 | C-H of cellulose |
| 2918 | 2917 | 2917 | 2917 | C-H of cellulose |
| 3318 | 3337 | 3338 | 3339 | O-H of cellulose |

## 4. X-Ray Diffraction Characterization of Cellulose

XRD diffractograms of cellulose samples (Figure 5) show characteristic peaks at approximately 2θ = 15°, 22°, and 35°. The broad peak near 15° corresponds to amorphous region, while the sharper peaks at around 22° and 35° represent crystalline regions, particularly cellulose I [39]. These results are consistent with previous study reporting typical cellulose I peaks near 2θ = 16°, 22°, and 35° [9]. The preservation of these peaks across all NaOH concentrations, without noticeable shifts, indicates that the fundamental crystalline structure of cellulose was largely maintained during alkali treatment under MAE [40]. This suggests that non-cellulosic components were removed without significantly altering the crystalline arrangement of cellulose microfibrils, which is important for maintaining mechanical and physicochemical properties [41].

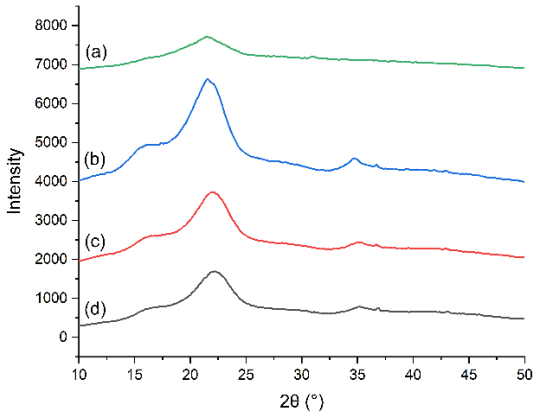


**Figure 5.** XRD diffractogram of (a) raw material, (b) Cellulose 1 (NaOH 4%), (c) Cellulose 2 (NaOH 8%), and (d) Cellulose 3 (NaOH 10%).

Cellulose 1 exhibited a more intense peak intensity at 2θ ≈ 22°, indicating a relatively higher degree of structural order. Crystallinity indices of Cellulose 1, Cellulose 2, and Cellulose 3 were 52.5%, 51.8%, and 40.3%, respectively, all higher than that of the raw material (10.1%), reflecting the removal of amorphous components [41]. This trend is consistent with the compositional analysis showing reduced lignin content in all samples.

Cellulose 2 showed a relatively high cellulose content (76.51%) and low lignin content (8.47%), its crystallinity index (51.8%) was slightly lower than that of Cellulose 1 (52.5%). This indicates that maximum cellulose purity does not necessarily correspond to maximum crystallinity. Crystallinity is influenced not only by the removal of amorphous components but also by structural rearrangement during alkaline treatment [42]. At higher alkali concentrations, partial cellulose degradation may occur [30][31], whereas moderate concentrations (4–8%) can remove non-cellulosic components while maintaining chain order through intra- and intermolecular hydrogen bonds and van der Waals interactions [9]. In contrast, at 10% NaOH, the lower crystallinity (40.3%) is accompanied by decreased cellulose content (72.44%) and increased lignin content (10.76%), suggesting a disruption of the ordered structure.

The evaluation indicates that the most suitable condition depends on the selected criterion. Cellulose 1 exhibited a slightly higher crystallinity index, suggesting a more ordered structure that may be advantageous for applications requiring high mechanical strength and thermal stability [43],[44]. In contrast, Cellulose 2 showed relatively high cellulose content and low lignin content, reflecting a higher degree of purity [45]. This distinction suggests that structural order and compositional purity do not necessarily reach their maxima under identical treatment conditions. Therefore, while 4% NaOH appears more favorable for achieving higher crystallinity, 8% NaOH may be considered a particularly favorable condition under the criteria applied in this study.

## 5. Morphological Characterization of Cellulose

The surface morphology of the isolated cellulose was examined using scanning electron microscopy (SEM), as shown in Figure 6. The analysis focused on the sample treated with 8% NaOH, which was selected based on the criteria applied.

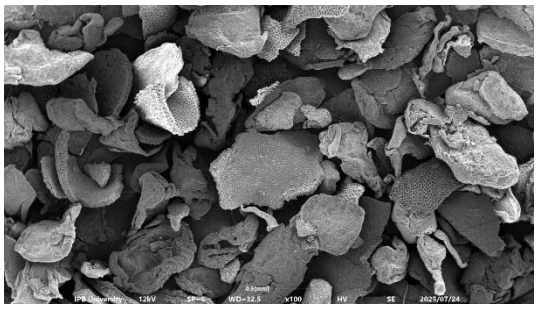

**Figure 6.** SEM image of cellulose treated with 8% NaOH (x100, 12 kV, WD 32.5 mm), showing fragmented and porous morphology associated with the removal of lignin and hemicellulose.

The SEM image shows irregular and fragmented structures with rough and heterogeneous surfaces. The particles appear as aggregated flakes of varying sizes, indicating disruption of the original compact plant matrix [46]. The presence of porous and

partially honeycomb-like features suggests that alkaline treatment may have removed amorphous components, particularly lignin and hemicellulose, thereby potentially exposing the internal structure of cellulose [47][48]. These observations are consistent with the compositional analysis and FTIR results, which indicate the removal of non-cellulosic components.

SEM analysis was limited to the 8% NaOH sample, these morphological observations should be interpreted with caution and cannot be generalized to all treatment conditions. Nevertheless, they provide qualitative evidence, suggesting that alkaline treatment under MAE may contributed to the removal of non-cellulosic components and to changes in biomass structure. These findings are also appear to be consistent with the XRD results, where increased crystallinity reflects improved structural order.

## CONCLUSION

This study demonstrates that microwave-assisted extraction (MAE) can be an effective method for isolating cellulose from golden melon peel. Among the tested conditions, 8% NaOH provided favorable results based on the criteria examined, yielding relatively high cellulose recovery and improved purity, as indicated by higher cellulose content and lower lignin content. FTIR and XRD analyses suggested the removal of non-cellulosic components and the preservation of the cellulose I structure. The crystallinity indices at 4% and 8% NaOH were comparable, indicating that structural order can be maintained within this concentration range. SEM analysis of the 8% NaOH sample further suggested disruption of the lignocellulosic matrix after treatment.

## REFERENCES

[1] R. S. Riseh, M. G. Vazvani, M. Hassanisaadi, and V. K. Thakur, “Agricultural wastes: A practical and potential source for the isolation and preparation of cellulose and application in agriculture and different industries,” *Ind. Crops Prod.*, vol. 208, p. 117904, 2024. [Online]. Available: https://doi.org/10.1016/j.indcrop.2023.117904

[2] T. Garg, S. Arora, and R. Pahwa, “Cellulose and its derivatives: Structure, modification, and application in controlled drug delivery,” *Futur. J. Pharm. Sci.*, vol. 11, p. 76, 2025. [Online]. Available: https://doi.org/10.1186/s43094-025-00834-2

[3] D. Trache, A. F. Tarchoun, M. Derradji, T. S. Hamidon, N. Masruchin, and N. Brosse, *et al.,* “Nanocellulose: From fundamentals to advanced applications,” *Front. Chem.*, vol. 8, art. 392, pp. 1–33, 2020. [Online]. Available: https://doi.org/10.3389/fchem.2020.00392

[4] E. Erniati, H. Suhardiyanto, R. Hasbullah, and S. Supriyanto, “Artificial neural networks to predict melon (*Cucumis melo* L.) production in tropical greenhouse, Indonesia,” *J. Keteknikan Pertan.*, vol. 11, no. 2, pp. 193–204, 2023. [Online]. Available: https://doi.org/10.19028/jtep.011.2.193-204

[5] R. Gómez-García, D. A. Campos, A. Oliveira, C. N. Aguilar, A. R. Madureira, and M. Pintado, “A chemical valorisation of melon peels towards functional food ingredients: Bioactives profile and antioxidant properties,” *Food Chem.*, vol. 335, p. 127579, 2021. [Online]. Available: https://doi.org/10.1016/j.foodchem.2020.127579

[6] T. Makaveckas, A. Šimonėlienė, and V. Šipailaitė-Ramoškienė, "Lignin valorization from lignocellulosic biomass: Extraction, depolymerization, and applications in the circular bioeconomy," *Sustainability*, vol. 17, no. 21, p. 9913, 2025. [Online]. Available: https://doi.org/10.3390/su17219913

[7] R. Gómez-García, S. C. Sousa, O. L. Ramos, D. A. Campos, C. N. Aguilar, and A. R. Madureira, *et al.,* "Obtention and characterization of microcrystalline cellulose from industrial melon residues following a biorefinery approach," *Molecules*, vol. 29, no. 14, p. 3285, 2024. [Online]. Available: https://doi.org/10.3390/molecules29143285

[8] A. Adewuyi and F. V. Pereira, "Isolation and characterization of cellulose from underexploited golden melon skin," *Makara J. Sci.*, vol. 22, no. 3, pp. 121–126, 2018. [Online]. Available: https://doi.org/10.7454/mss.v22i3.7548

[9] N. P. Yupa, H. Purwaningsih, and T. Kemala, "Synthesis and characterization of corn husk (Zea mays L.) cellulose using microwave-assisted extraction (MAE)," *J. Kim. Sains Apl.*, vol. 26, no. 7, pp. 268–275, 2023. [Online]. Available: https://doi.org/10.14710/jksa.26.7.268-275

[10] E. Dan, A. J. McCue, D. Dionisi, and C. Fernández Martín, "On the potential of microwave heating to convert waste into added-value chemicals and materials: A review," *Philos. Trans. A Math. Phys. Eng. Sci.*, vol. 383, no. 2297, p. 20240071, 2025. [Online]. Available: https://doi.org/10.1098/rsta.2024.0071

[11] A. Bahndral, R. Shams, K. K. Dash, N. A. Ali, A. M. Shaikh, and B. Kovács, "Microwave assisted extraction of cellulose from lemon grass: Effect on techno-functional and microstructural properties," *J. Agric. Food Res.*, vol. 16, p. 101170, 2024. [Online]. Available: https://doi.org/10.1016/j.jafr.2024.101170

[12] A. Valdés, G. Mondragon, M. C. Garrigós, A. Eceiza, and A. Jiménez, "Microwave-assisted extraction of cellulose nanocrystals from almond (*Prunus amygdalus*) shell waste," *Front. Nutr.*, vol. 9, p. 1071754, 2022. [Online]. Available: https://doi.org/10.3389/fnut.2022.1071754

[13] Q. Ji, X. Yu, A. E.-G. A. Yagoub, L. Chen, and C. Zhou, "Efficient removal of lignin from vegetable wastes by ultrasonic and microwave-assisted treatment with ternary deep eutectic solvent," *Ind. Crops Prod.*, vol. 149, p. 112357, 2020. [Online]. Available: https://doi.org/10.1016/j.indcrop.2020.112357

[14] Y. Mao, A. Gerrow, E. Ray, N. D. Perez, K. Edler, and B. Wolf, *et al.,* "Lignin recovery from cocoa bean shell using microwave-assisted extraction and deep eutectic solvents," *Bioresour. Technol.*, vol. 372, p. 128680, 2023. [Online]. Available: https://doi.org/10.1016/j.biortech.2023.128680

[15] E. Şen, E. Göktürk, and E. Uğuzdoğan, "Microwave-assisted extraction of pectin from onion and garlic waste under organic, inorganic and dual acid mixtures," *Food Meas.*, vol. 18, pp. 3189–3198, 2024. [Online]. Available: https://doi.org/10.1007/s11694-024-02395-z

[16] I. Iliyin, H. Purwaningsih, and T. T. Irawadi, "Isolation and characterization of cellulose from banana stems using microwave heating," *Jurnal Kimia Valensi*, vol. 6, no. 2, pp. 169–176, 2020. [Online]. Available: https://doi.org/10.15408/jkv.v6i2.15962

[17] ASTM International, *ASTM D1103-60 – Standard Test Method for Alpha-Cellulose in Wood*. West Conshohocken, PA, USA: ASTM International, 1977.

[18] Badan Standardisasi Nasional, *SNI 8429:2017 – Penentuan Kadar Lignin – Metode Klason*. Jakarta, Indonesia: BSN, 2017.

[19] D. E. S. Souza, J. J. Melo, F. F. Santos, A. L. Vasconcelos, A. D. Jesus, L. D. Freitas, et al., "Microwave-assisted vs. conventional extraction of Moringa oleifera seed oil: Process optimization and efficiency comparison," *Foods*, vol. 13, no. 19, art. 3141, pp. 1–15, 2024. [Online]. Available: https://doi.org/10.3390/foods13193141

[20] W. Chen, Q. Zhang, X. Lin, K. Jiang, and D. Han, "The degradation and repolymerization analysis on solvolysis liquefaction of corn stalk," *Polymers*, vol. 12, no. 10, pp. 1–13, 2020. [Online]. Available: https://doi.org/10.3390/polym12102337

[21] Q. Zhou, A. Ding, L. Zhang, J. Wang, J. Gu, and T. Y. Wu, *et al.,* "Furfural production from the lignocellulosic agro-forestry waste by solvolysis method – A technical review," *Fuel Process. Technol.*, vol. 255, p. 108063, 2024. [Online]. Available: https://doi.org/10.1016/j.fuproc.2024.108063

[22] R. K. Wardani, H. Holilah, H. Bahruji, Z. A. A. Hamid, S. Suprapto, A. A. Jalil, et al., "The comparison of hydrothermal, ultrasonication and microwave assisted alkalization of cellulose from *Borassus flabellifer* fruit husk," *Sustain. Chem. Pharm.*, vol. 39, pp. 1–11, 2024. [Online]. Available: https://doi.org/10.1016/j.scp.2024.101583

[23] K. Q. T. Doan and K. Y. Chiang, "Statistical optimization of cellulose nanocrystal from cotton cloth waste using sulfuric acid hydrolysis and response surface methodology," *Int. J. Environ. Sci. Technol.*, vol. 21, no. 1, pp. 5691–5704, 2024. [Online]. Available: https://doi.org/10.1007/s13762-023-05384-9

[24] S. Zhao, X. Chen, Z. Fan, R. Ni, X. Liu, Y. Tian, and B. Zhou, "Using lignin degraded to synthesize phenolic foams with excellent flame retardant property," *Colloids Surf. A Physicochem. Eng. Asp.*, vol. 666, art. 131373, pp. 1–9, 2023. [Online]. Available: https://doi.org/10.1016/j.colsurfa.2023.131373

[25] J. Li, Y.-N. Zha, H.-M. Wang, J.-N. Tian, and Q.-X. Hou, "Advances in lignin chemistry during pulping and bleaching," *Ind. Crops Prod.*, vol. 229, p. 121004, 2025. [Online]. Available: https://doi.org/10.1016/j.indcrop.2025.121004

[26] K. J. Nagarajan, N. R. Ramanujam, M. R. Sanjay, S. Siengchin, B. S. Rajan, K. S. Basha, P. Madhu, and G. R. Raghav, "A comprehensive review on cellulose nanocrystals and cellulose nanofibers: Pretreatment, preparation, and characterization," *Polym. Compos.*, vol. 42, no. 4, pp. 1588–1630, 2021. [Online]. Available: https://doi.org/10.1002/pc.25929

[27] C. Long, C. Rösch, S. de Vries, H. Schols, and K. Venema, "Correction to cellulase and alkaline treatment improve intestinal microbial degradation of recalcitrant fibers of rapeseed meal in pigs," *J. Agric. Food Chem.*, vol. 68, no. 52, p. 15535, 2020. [Online]. Available: https://doi.org/10.1021/acs.jafc.0c07502

[28] X. Sun, Y. Su, Y. Hao, J. Zhang, X. Yue, and W. Wang, et al., "Novel process methods for the whole cottonseed: Effect on the digestibility, productivity, fat profile, and milk gossypol levels in lactating dairy cows," *Front. Nutr.*, vol. 9, p. 801712, 2022. [Online]. Available: https://doi.org/10.3389/fnut.2022.801712

[29] H. Wang, M. Shi, Z. Ma, X. Zhang, H. Shan, and X. Xu, et al., "Metabolomics study revealed the effects of CaO-treated maize straw on the rumen metabolites," *Animals*, vol. 15, no. 5, p. 674, 2025. [Online]. Available: https://doi.org/10.3390/ani15050674

[30] I. Kurniaty, U. H. Habibah, D. Yustiana, and I. M. Fajriah, "Proses delignifikasi menggunakan NaOH dan amonia ($NH_3$) pada tempurung kelapa," *J. Integr. Pros.*, vol. 6, no. 4, pp. 197–201, 2017. [Online]. Available: https://doi.org/10.36055/jip.v6i4.2546

[31] B. Irawan, A. Darmawan, A. Roesyadi, and D. H. Prajitno, "Improving reaction selectivity with NaOH charges and reaction time in the medium consistency oxygen delignification process," *Int. J. Technol.*, vol. 11, no. 4, pp. 764–773, 2020. [Online]. Available: https://doi.org/10.14716/ijtech.v11i4.3499

[32] C. Zheng, J. W. Cone, A. van Peer, J. J. P. Baars, and W. H. Hendriks, "Conversion of lignocellulosic biomass into valuable feed for ruminants using white rot fungi," *J. Anim. Physiol. Anim. Nutr.*, vol. 109, no. 3, pp. 800–811, 2025. [Online]. Available: https://doi.org/10.1111/jpn.14099

[33] H. R. Permatasari, F. Gulo, and B. Lesmini, "Pengaruh konsentrasi $H_2SO_4$ dan NaOH terhadap delignifikasi serbuk bambu (*Gigantochloa apus*)," *J. Penelit. dan Pendidik. Kim.*, vol. 1, no. 2, pp. 131–140, 2014. [Online]. Available: https://doi.org/10.36706/jppk.v1i2.1891

[34] R. Javier-Astete, J. Jimenez-Davalos, and G. Zolla, "Determination of hemicellulose, cellulose, holocellulose and lignin content using FTIR in *Calycophyllum spruceanum* (Benth.) K. Schum. and *Guazuma crinita* Lam.," *PLoS One*, vol. 16, no. 10, p. e0256559, 2021. [Online]. Available: https://doi.org/10.1371/journal.pone.0256559

[35] F. Meng, G. Wang, X. Du, Z. Wang, S. Xu, and Y. Zhang, "Extraction and characterization of cellulose nanofibers and nanocrystals from liquefied banana pseudo-stem residue," *Compos. B Eng.*, vol. 160, pp. 341–347, 2018. [Online]. Available: https://doi.org/10.1016/j.compositesb.2018.08.048

[36] A. Boukir, S. Fellak, and P. Doumenq, "Structural characterization of *Argania spinosa* Moroccan wooden artifacts during natural degradation progress using infrared spectroscopy (ATR-FTIR) and X-ray diffraction (XRD)," *Heliyon*, vol. 5, no. 9, p. e02477, 2019. [Online]. Available: https://doi.org/10.1016/j.heliyon.2019.e02477

[37] S. Biswas, T. Rahaman, P. Gupta, R. Mitra, S. Dutta, E. Kharlyngdoh, et al., "Cellulose and lignin profiling in seven, economically important bamboo species of India by anatomical, biochemical, FTIR spectroscopy and thermogravimetric analysis," *Biomass Bioenerg.*, vol. 162, p. 106362, 2022. [Online]. Available: https://doi.org/10.1016/j.biombioe.2022.106362

[38] A. Singh, B. Ranawat, and R. Meena, "Extraction and characterization of cellulose from halophytes: Next generation source of cellulose fibre," *SN Appl. Sci.*, vol. 1, p. 1311, 2019. [Online]. Available: https://doi.org/10.1007/s42452-019-1160-6

[39] N. Montoya-Escobar, D. Ospina-Acero, J. A. Velásquez-Cock, C. Gómez-Hoyos, A. S. Guerra, P. F. G. Rojo, et al., "Use of Fourier series in X-ray diffraction (XRD) analysis and Fourier-transform infrared spectroscopy (FTIR) for estimation of crystallinity in cellulose from different sources," *Polymers*, vol. 14, no. 23, pp. 1–16, 2022. [Online]. Available: https://doi.org/10.3390/polym14235199

[40] A. F. Tarchoun, D. Trache, T. M. Klapötke, M. Derradji, and W. Bessa, "Ecofriendly isolation and characterization of microcrystalline cellulose from giant reed using various acidic media," *Cellulose*, vol. 26, no. 1, pp. 7635–7651, 2019. [Online]. Available: https://doi.org/10.1007/s10570-019-02672-x

[41] P. S. Rai, S. Unnikrishnan, and A. Chandrashekar, "Influence of alkali treatment on physicochemical and morphological properties of palmyra fibers," *Ind. Crops Prod.*, vol. 224, p. 120298, 2025. [Online]. Available: https://doi.org/10.1016/j.indcrop.2024.120298

[42] M. H. Mulla, M. N. Norizan, N. F. M. Rawi, M. H. M. Kassim, N. Abdullah, and M. N. F. Norrrahim, "Surface and

interfaces effects of concentrations and alkaline treatment durations on sugar palm fiber as structural reinforcement in polymer composites," *J. Nat. Fibers*, vol. 22, no. 1, p. 2527277, 2025. [Online]. Available: https://doi.org/10.1080/15440478.2025.2527277

[43] V. Balasubramani, K. J. Nagarajan, M. Karthic, and R. Pandiyarajan, "Extraction of lignocellulosic fiber and cellulose microfibrils from agro waste-palmyra fruit peduncle: Water retting, chlorine-free chemical treatments, physio-chemical, morphological, and thermal characterization," *Int. J. Biol. Macromol.*, vol. 259, pt. 2, p. 129273, 2024. [Online]. Available: https://doi.org/10.1016/j.ijbiomac.2024.129273

[44] S. Zidi, "Cellulose of sisal fibers integration in papermaking: Mechanical and thermal characterization," *Multiscale Multidiscip. Model. Exp. Des.*, vol. 8, p. 73, 2025. [Online]. Available: https://doi.org/10.1007/s41939-024-00673-3

[45] S. Srinivasan and S. Venkatachalam, "One pot green process for facile fractionation of sorghum biomass to lignin, cellulose and hemicellulose nanoparticles using deep eutectic solvent," *Int. J. Biol. Macromol.*, vol. 277, pt. 3, p. 134295, 2024. [Online]. Available: https://doi.org/10.1016/j.ijbiomac.2024.134295

[46] P. T. H. Anh and D. M. Tai, "Closer approach towards the preparation of cellulose and microcrystalline cellulose from corn husks," *Chem. Eng. Technol.*, vol. 47, no. 9, p. e202300379, 2024. [Online]. Available: https://doi.org/10.1002/ceat.202300379

[47] J. Pu, T. Huhe, X. Ding, R. Yuan, S. Zhang, and J. Ren, et al., "Co-production of polysaccharides and platform sugars from wheat straw fermented with *Irpex lacteus*," *Sustainability*, vol. 17, no. 10, p. 4581, 2025. [Online]. Available: https://doi.org/10.3390/su17104581

[48] P. Rani, C. Ram, A. Yadav, D. K. Yadav, K. Bishnoi, and N. R. Bishnoi, "Comparative analysis of various seed sludges for biohydrogen production from alkaline pretreated rice straw," *Nat. Environ. Pollut. Technol.*, vol. 23, no. 2, pp. 1065–1073, 2024. [Online]. Available: https://doi.org/10.46488/NEPT.2024.v23i02.040